This is a peer-reviewed, author's accepted manuscript of the following conference proceedings paper: Borg, M. G., DeMarco Muscat-Fenech, C., Tezdogan, T., Sant, T., Mizzi, S., & Demirel, Y. K. (2022). Numerically analysing liquid-cargo sloshing diminishment in partitioned rectangular tanks. In *ASME 2022 41st International Conference on Ocean, Offshore and Arctic Engineering* (Vol. 7). [OMAE2022-86100]
ASME. https://doi.org/10.1115/omae2022-86100

NUMERICALLY ANALYSING LIQUID-CARGO SLOSHING DIMINISHMENT IN PARTITIONED RECTANGULAR TANKS

Mitchell G. Borg
Department of Mechanical Engineering,
University of Malta
Msida, Malta

Claire DeMarco Muscat-Fenech
Department of Mechanical Engineering,
University of Malta
Msida, Malta

Tahsin Tezdogan
Department of Naval Architecture, Ocean, and Marine Engineering,
University of Strathclyde
Glasgow, United Kingdom

Tonio Sant
Department of Mechanical Engineering,
University of Malta
Msida, Malta

Simon Mizzi
Department of Mechanical Engineering,
University of Malta
Msida, Malta

Yigit Kemal Demirel
Department of Naval Architecture, Ocean, and Marine Engineering,
University of Strathclyde
Glasgow, United Kingdom

ABSTRACT

This study puts forward an analysis of the influence of liquid sloshing upon oscillating vessels by means of numerical modeling. Rectangular cross-sectional tanks incorporating an open-bore and partitioned setups at 20%, 40%, and 60% fill-volume levels were implemented to establish the torque and static pressure exerted solely by the fluid dynamics upon oscillation within the tanks. Through verification of dam-break dynamics, the sloshing models coupled the explicit volume-of-fluid and non-iterative time-advancement schemes within a computational fluid dynamic solver. Utilising an oscillatory frequency of 1 Hz, the resultant liquid impact reduced within the partitioned setup due to the suppression of wave dynamics.

Keywords: sloshing, pendulum-tank oscillation, rectangular tank, CFD, NITA, VOF.

NOMENCLATURE

A_t	tank frontal area
B_c	channel breadth
B_t	tank breadth
B_r	reservoir breadth
C_Q	torque coefficient
C_P	pressure coefficient
g	gravitational acceleration
H_c	channel height
H_t	tank height
H_r	reservoir height
L_c	channel length
L_t	tank length
L_r	reservoir length
P	static pressure
Q	torque
t	time
U_w	wave-front celerity
ρ	fluid density
θ_t	oscillatory displacement
μ	fluid viscosity

1. INTRODUCTION

Throughout transportation of liquid cargo within partially-filled tanks along shipping routes, violent ship motions due to adverse weather conditions may induce substantial dynamic variation upon the contained cargo, detrimentally affecting vessel seakeeping and manoeuvrability. Attributable to the partially-filled multiphase domain, external forces acting upon the vessel tank shift the liquid-phase from an equilibrium state, displacing the centre of mass and free-surface, characterising the sloshing phenomenon [1]. Significant sloshing dynamics within liquefied natural gas (LNG) cargo tanks materialise as breaking waves that potentially bring about containment structural damage and stability loss due to high-impact slamming [2,3]. In

accordance, tank-fill limitations have been acknowledged as precautions to prevent engineering repercussions due to sloshing, imposing cargo volume-fill limitations to be either lower than 10% or higher than 70% of the tank height [2]. The restrictions, however, limit commercial transactions, distinctively when handling spot trades and offshore loading/unloading at multiple ports along a shipping route.

In utilising linear theoretical sloshing analysis, Budiansky [4] established that the fundamental frequency of the sloshing dynamics increased in a monotonic manner with increasing fill-volumes for fill-levels of less than 60%, yet attained an increased rate-of-change at higher fills. Abramson [5] correspondingly concluded the tank fill-volume to be a contributing factor in establishing the natural frequency of the liquid-slosh motion for various tank configurations. Considering sloshing investigations by means of a pendulum-equivalent mechanical system model, Slibar and Troger [6] studied liquid sloshing utilising a single degree-of-freedom mechanical oscillator to compute the fluid dynamics. Further, Ranganathan [7] modelled large-amplitude non-linear liquid-sloshing within horizontal partially-filled cylindrical cargo-tanks coupled with dynamic roll accelerations, whereas Salem et al. [8] indicated the magnitude of the accelerations induced to be a characteristic factor in the liquid-response.

In establishing a computational fluid dynamic (CFD) methodology for seafaring sloshing investigations, Celebi and Akyildiz [9] investigated non-linear liquid sloshing inside a partially-filled rectangular tank. Tank kinetics were induced harmonically to simulate rolling motion. The model solved the Navier–Stokes equations by implementing finite-difference approximations, whilst utilising the volume-of-fluid (VOF) technique to track the free surface. In continuation, Akyildiz [10] investigated the roll dynamics of a partially-filled rectangular tank with a vertical baffle by varying the ratio of baffle height to initial liquid depth. Bulian et al. [11] developed a six degree-of-freedom (DOF) ship motion numerical solver by coupling rigid-body dynamics and external fluid-structure interaction with a smoothed-particle hydrodynamics solver to analyse the internal sloshing dynamics. Thiagarajan et al. [12] carried out numerical investigations on sloshing motions in a two-dimensional tank with fill-levels varying from 10% to 95% of the tank height, an oscillation frequency range of 0.35 Hz to 1.25 Hz, and a peak-to-peak displacement of 0.25 m. Utilising the finite-volume method coupled with the VOF technique, the computational results for free-surface elevation and impact pressure were found to be in good agreement with experimentation.

The implementation of partitions within a rectangular containment unit for the purpose of sloshing suppression has been widely established to be of particular interest due to its practical large-scale use and cost-effective simplicity in fabrication and installation. Yet, albeit the undertaken research, the efficacy of installing partitions as tank architecture for slosh suppression by utilising high-fidelity numerical modelling has not been undertaken. Moreover, literature has elaborated slosh dampening in terms of free-surface reduction and localised wall-pressure diminishment, yet utilising a pendulum model to determine the holistic torque variation induced by the fluid within the tank, rather than solely a qualitative or localised-quantitative data analysis, has not been tackled [13]. For this reason, this research tackles a three-dimensional VOF-CFD approach, utilising the non-iterative time-advancement (NITA) technique, in modelling the dynamic sloshing torque within an open-bore & partitioned rectangular containment unit when undergoing simple harmonic oscillatory motion.

2. NUMERICAL METHODOLOGY

2.1 Physical Setup

In an effort to attain a validated numerical model for sloshing applications, simulations were established to numerically replicate theoretical values of an instantaneous turbulent dam break in a dry rectangular horizontal channel put forward by Chanson [14]. The general dimensions of the channel included a length (L_c), height (H_c), and breadth (B_c) of 30 m, 0.30 m, and 0.60 m, respectively. Within the channel, the initially-static water reservoir dimensions included a length (L_r), height (H_r), and breadth ($B_r = 4H_r$) of 15 m, 0.15 m, and 0.60 m, respectively, attaining a Reynolds number of 1.81×10^5. The channel dimensions were implemented to acquire a wide semi-infinite reservoir with an analogous breadth-to-height cross-sectional length-scale to the sloshing tanks designed. The transient model was solved once the wave reached the channel end, approximately equivalent to 13 seconds, to attain an analogous time-scale to the oscillating tank model.

In continuation, the tank geometrical models described two distinct setups: an open-bore tank and a partitioned tank. The dimensions of the tanks described a length (L_t), height (H_t), and breadth (B_t) of 0.48 m, 0.23 m, and 0.20 m, respectively, as illustrated in Figure 1. Truncations at the tank length-to-height cross-section corners were imposed 0.05 m from the vertex at a 45° angle. The dimensions replicated physical experimentation conducted with a 2:1 length-to-height cross-sectional aspect ratio tank of 0.50 m by 0.25 m by 0.22 m, with a 10 mm tank-wall thickness. The partitioned tank model imposed a partition plate of 10 mm thickness along the vertical symmetrical plane, as displayed in Figure 2. The oscillatory kinematics were considered from guidelines published by Det Nørske Veritas (DNV) [2] and Ship Structure Committee (SSC) [15] that established oscillation amplitudes for cargo hold tanks undergoing roll of 4°, 7.5°, 15°, and 30° at a maximum resonant frequency, in relation to the tank properties currently utilised, of 1.08 Hz. In recognition, parameters related to the three tank models at 20%, 40%, and 60% fills within a maximum oscillatory displacement (θ_t) of 15° at a frequency of 1.0 Hz were implemented.

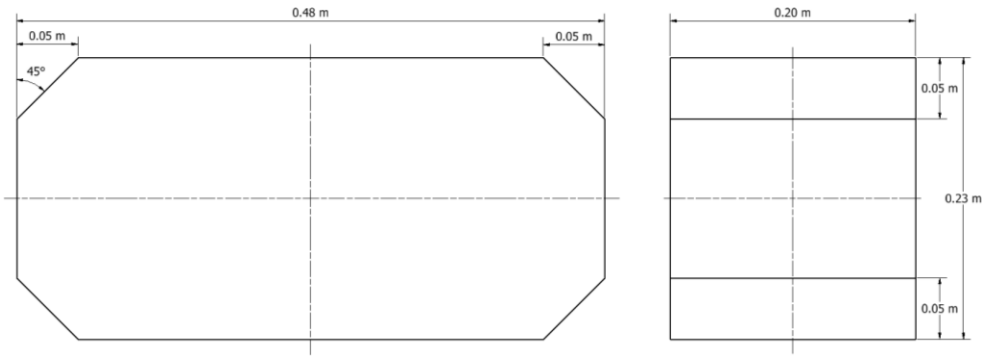

FIGURE 1: FIRST-ANGLE PROJECTION OF THE OPEN-BORE TANK GEOMETRICAL MODEL

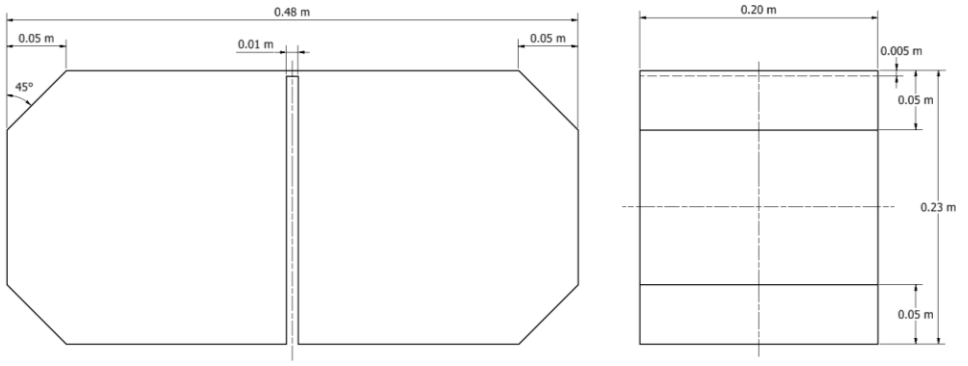

FIGURE 2: FIRST-ANGLE PROJECTION OF THE PARTITIONED TANK GEOMETRICAL MODEL

2.2 Computational Setup

The dam-break channel and sloshing-tank numerical models were solved utilising the VOF-CFD (volume-of-fluid computational fluid dynamics) methodology to track the multiphase free-surface. The commercial solver ANSYS Fluent 19.2 was utilised in computing the continuity and Navier-Stokes equations. The Shear-Stress Transport (SST) k-ω Unsteady Reynolds-Averaged Navier-Stokes (URANS) turbulence model was implemented in mathematical closure to represent flow property fluctuation within the three-dimensional unsteady flow field.

The VOF scheme was utilised with Explicit formulation volume fraction parameters, Sharp interface, and surface tension modelling. The non-iterative time-advancement (NITA) algorithm was utilised to diminish the total solution time [16]. The Fractional Step pressure-velocity coupling scheme was implemented with the Green-Gauss Node Based gradient, Pressure Staggering Option pressure, Second Order Upwind momentum, Geo-Reconstruct volume fraction, Second Order Upwind turbulent kinetic energy, and Second Order Upwind specific dissipation rate spatial discretisation schemes. The First Order Implicit transient formulation scheme was utilised as the Explicit VOF model was implemented; second order models were hence inapplicable. The simulation time-step (Δt_{step}) was set to vary in relation to a model Courant number of 2.

The full numerical domain of the dam-break wave represented the channel & reservoir. The no-slip wall condition was implemented upon the channel bed and rear plane. The pressure-outlet condition was allocated to the top and front planes. The symmetry condition was applied to the side planes. The domain was segregated into two cell-zones for distinct phase implementation. The tank domain surfaces were applied with the no-slip wall condition. Volumetric variations for phase implementation was induced within the solver by allocating distinct regions within the domain. Oscillatory kinetics were induced in the form of the simple pendulum equation of motion to numerically replicate a simple harmonic oscillator by means of a user-defined function (UDF) within a moving-mesh model. Furthermore, to establish sloshing impact zones, as defined in the International Towing Tank Conference (ITTC) sloshing guidelines [17], the tank geometric model surfaces were split at the vertices to establish regions, illustrated in Figure 3, within which area-averaged static pressure data was acquired.

A mesh independence procedure was carried out on the tank, establishing a total mesh count equivalent to 1,008,640 hexahedral volumetric cells. Figure 3 presents an illustration of the tank mesh utilised for the computational fluid dynamic analysis. The final mesh was implemented with an initial cell-height to achieve a y-plus value of $30 < y^{+} < 300$ across the tank inner walls.

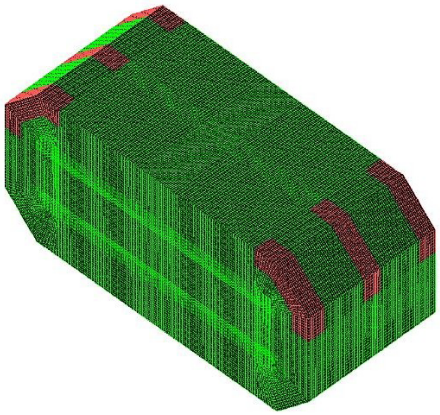

FIGURE 3: MESHED REPRESENTATION OF THE OPEN-BORE TANK WITH HIGHLIGHTED SURFACE ZONES FOR AREA-AVERAGED STATIC PRESSURE DATA ACQUISITION

2.3 Physical Modelling

In establishing the validation model, the theoretical values for the dam-break wave-tip displacement and instantaneous free-surface wave profiles were acquired as derived by Chanson [14]. The frontal wave-tip displacement (x_s) was defined as:

$$x_s = H_r \left(\frac{3}{2}\frac{U_w}{\sqrt{gH_r}} - 1\right)\sqrt{\frac{g}{H_r}}\,t + \frac{1}{32}\left(\frac{2.5\times10^{-3}}{Re_{H_r}}\right)^{\frac{1}{4}}\left(\frac{U_w}{\sqrt{gH_r}}\right)^{-2}\left(1 - \frac{U_w}{\sqrt{gH_r}}\right)^{\frac{1}{9}} \quad (1)$$

where H_r is the initial reservoir height, U_w is the wave-front celerity, g is the acceleration due to gravity, t is the elapsed time, $Re_{H_r} = \rho\sqrt{gH_r^3}/\mu$ is the dam-break Reynolds number, ρ is the fluid density, μ is the fluid viscosity.

The tank oscillatory displacement was attained within the CFD solver by imposing an oscillatory rotational velocity (ω_t):

$$\omega_t = \theta_t \cdot 2\pi f_n \cdot \cos(2\pi f_n t) \quad (2)$$

where θ_t is the oscillatory displacement, f_n is the oscillatory frequency, and t is the elapsed time.

In acknowledging sloshing motion within a rectangular cross-sectional tank, the sloshing torque coefficient (C_Q) was defined as:

$$C_Q = \frac{Q}{\rho g A_t L_t^2 \theta_t} \quad (3)$$

where Q is the torque generated by the fluid within the tank, and $A_t = L_t \cdot H_t$ is the frontal area of the tank.

Furthermore, the sloshing pressure coefficient (C_P) was defined as:

$$C_P = \frac{P}{\rho g L_t \theta_t} \quad (4)$$

where P is the static pressure generated by the fluid within the tank.

3. RESULTS AND DISCUSSION

3.1 Numerical Validation Modelling of a Turbulent Dam-Break Wave

In validation of the multiphase VOF-CFD model, the numerical outcomes of a three-dimensional turbulent dam break wave, acquiring the wave-tip displacement, were ascertained in comparison to theoretical values in Chanson [14] utilising the coefficient of determination (R^2) statistical methodology. The wave-tip displacement (x_s) numerical curve, illustrated in Figure 4, attained a coefficient of determination of 0.996 with the theoretical function, ascertaining very good comparison.

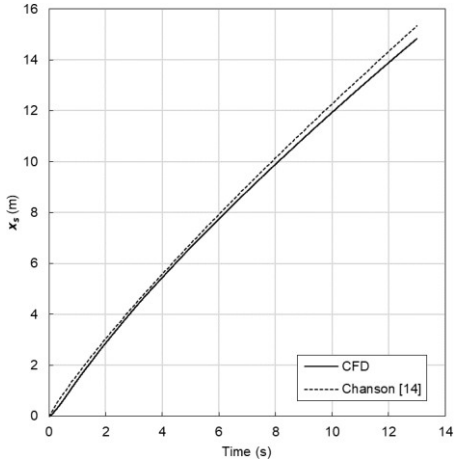

FIGURE 4: TURBULENT DAM-BREAK WAVE-TIP DISPLACEMENT (x_s) WITH TIME

3.2 Numerical Sloshing Modelling of an Open-Bore and Partitioned Tank

To establish the performance of utilising an open-bore and a partitioned tank, the cycle-averaged torque coefficient was analysed in relation to oscillation angle to determine acute output variations, notably due to breaking-wave slamming impact. Upon acknowledgement of slamming, the area-averaged static pressure from the critical locations speculated in Figure 3 of the two tank designs was acquired to verify sloshing suppression performance.

3.2.1 20% Fill

In analysing the resultant torque at 20% fill, the response output within the open-bore tank, illustrated in Figure 5, exhibited a sigmoidal variation with angular displacement, acquiring a peak coefficient of ±0.011 at the maximum angular displacement. Slamming due to breaking waves was not recognised. The output response within the partitioned tank

(Figure 6) similarly displayed a sigmoidal relationship with angular displacement, yet the coefficient rose to ±0.03 with an acute variation in the vicinity of the oscillation dead-centre.

The acute variation was induced due to the minor shift in the liquid-body, accumulating towards the partition walls. The open-bore response was acknowledged to be the lesser due to the momentum dissipation of the standing wave generated per half-cycle of the oscillation along the tank length. Due to the displacement suppression within the partitioned tank, the standing wave produced larger forces at the walls.

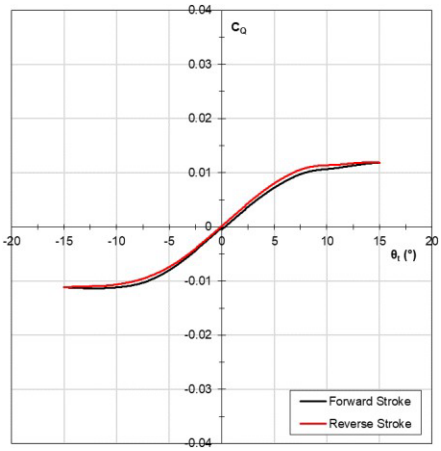

FIGURE 5: CYCLE-AVERAGED TORQUE COEFFICIENT (C_Q) WITH ANGULAR DISPLACEMENT (θ_t) OF THE OPEN-BORE TANK AT 20% FILL

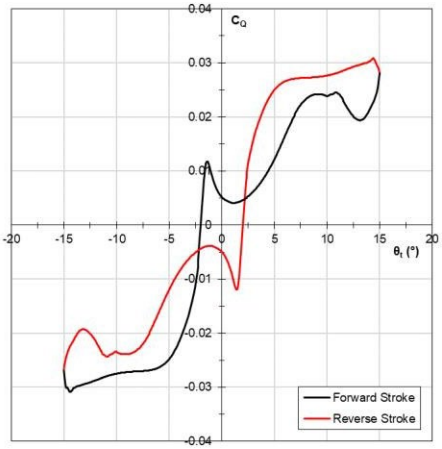

FIGURE 6: CYCLE-AVERAGED TORQUE COEFFICIENT (C_Q) WITH ANGULAR DISPLACEMENT (θ_t) OF THE PARTITIONED TANK AT 20% FILL

3.2.2 40% Fill

At 40% fill, the response output within the open-bore tank (Figure 7) exhibited a non-sigmoidal variation with angular displacement, acquiring a peak coefficient of ±0.11 at an angular displacement of ±10°. Slamming was acknowledged due to the acute increase in torque. The output response within the partitioned tank (Figure 8) displayed a sigmoidal relationship with angular displacement with a maximum coefficient rose of ±0.045, establishing the effective implementation in suppressing the sloshing wave momentum within the tank at the distinct frequency.

The static pressure coefficient at the tank roof locations was analysed due to the acute variation in torque. Illustrated in Figure 9, the area-averaged static pressure coefficient at the locations peaked twice to a maximum value of 0.13. verifying the slamming effect occurred twice per oscillation cycle.

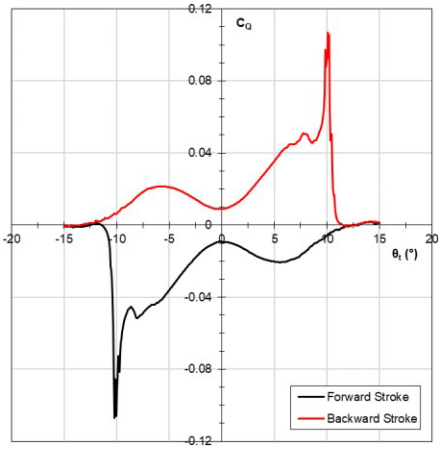

FIGURE 7: CYCLE-AVERAGED TORQUE COEFFICIENT (C_Q) WITH ANGULAR DISPLACEMENT (θ_t) OF THE OPEN-BORE TANK AT 40% FILL

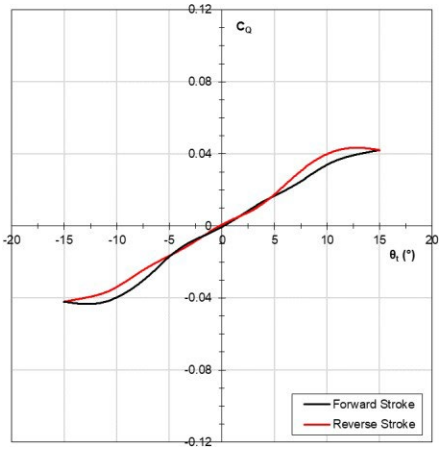

FIGURE 8: CYCLE-AVERAGED TORQUE COEFFICIENT (C_Q) WITH ANGULAR DISPLACEMENT (θ_t) OF THE PARTITIONED TANK AT 40% FILL

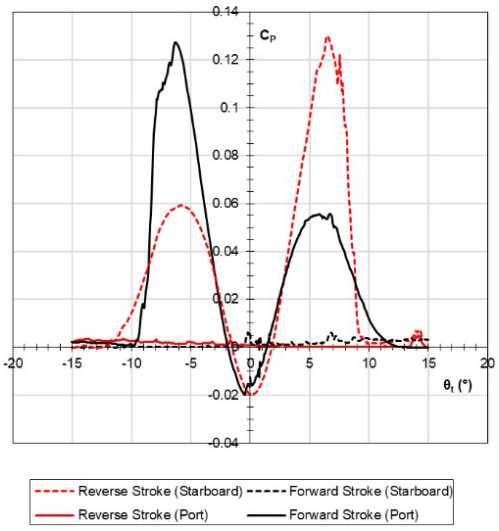

FIGURE 9: CYCLE-AVERAGED STATIC PRESSURE COEFFICIENT (C_P) WITH ANGULAR DISPLACEMENT (θ_t) OF THE OPEN-BORE TANK AT 40% FILL

3.2.3 60% Fill

At 60% fill, the response output within the open-bore tank (Figure 10) exhibited a non-sigmoidal variation with angular displacement, acquiring a peak coefficient of ±0.06 at an angle of ±5°. Subsequently, within one-third of a cycle, the torque coefficient varied to ±0.045, establishing a resultant torque discrepancy of 0.105. The substantial variation in magnitude and orientation of torque manifested due to the high-energy wave slamming with succeeded by a ricochet of the wave dynamics from one tank side to the opposite tank side. The output response within the partitioned tank (Figure 11) displayed a sigmoidal relationship with angular displacement with a maximum coefficient rose of ±0.048, further establishing the effective implementation in suppressing the sloshing wave momentum within the tank at the distinct frequency.

The static pressure coefficient at the tank roof locations was analysed due to the variation in torque. Illustrated in Figure 12, the area-averaged static pressure coefficient at the locations peaked twice to a maximum value of 0.26.

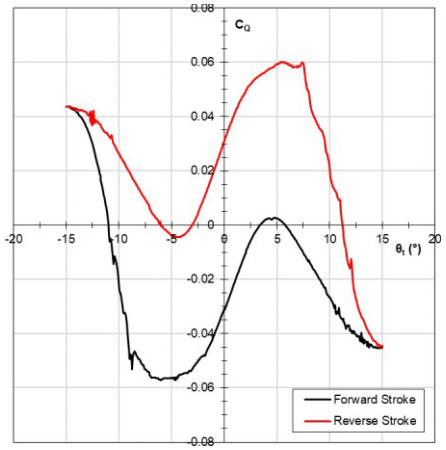

FIGURE 10: CYCLE-AVERAGED TORQUE COEFFICIENT (C_Q) WITH ANGULAR DISPLACEMENT (θ_t) OF THE OPEN-BORE TANK AT 60% FILL

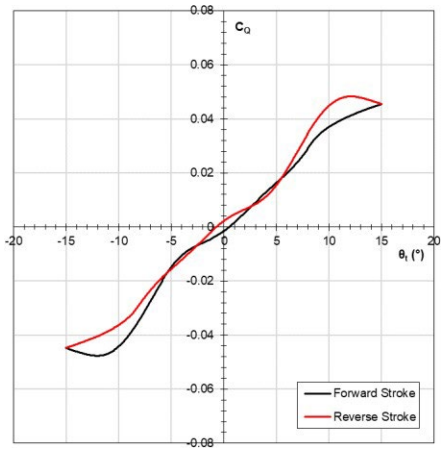

FIGURE 11: CYCLE-AVERAGED TORQUE COEFFICIENT (C_Q) WITH ANGULAR DISPLACEMENT (θ_t) OF THE PARTITIONED TANK AT 60% FILL

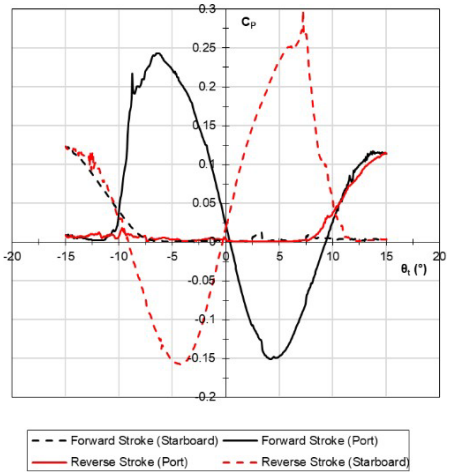

FIGURE 12: CYCLE-AVERAGED STATIC PRESSURE COEFFICIENT (C_P) WITH ANGULAR DISPLACEMENT (θ_t) OF THE OPEN-BORE TANK AT 60% FILL

4. CONCLUSION

This study put forward an analysis of the influence of liquid sloshing upon oscillating vessels by means of numerical modeling. Rectangular cross-sectional tanks incorporating an open-bore and partitioned setups at 20%, 40%, and 60% fill-volume levels were implemented to establish the torque and static pressure exerted solely by the fluid dynamics upon oscillation within the tanks.

Through verification of dam-break dynamics, the sloshing models coupled the explicit volume-of-fluid and non-iterative time-advancement schemes within a computational fluid dynamic solver. Utilising an oscillatory frequency of 1 Hz, the resultant slamming impact at the tank roof was reduced within the partitioned setup due to the physical suppression of the wave dynamics.

ACKNOWLEDGEMENTS

The research was funded by Malta Marittima and Transport Malta via the 'DeSloSH' project supported through the Maritime Seed Award 2020. Additionally, the research was funded as part of the European Union's Horizon 2020 research and innovation programme, VENTuRE (project no. 856887).

REFERENCES

[1] Olsen, H. What is Sloshing? In Seminar on Liquid Sloshing. Den Nørske Veritas (DNV): Hovik, Norway, 1976.

[2] Det Nørske Veritas (DNV). DNVGL-CG-0158 Sloshing analysis of LNG membrane tanks. Technical report. 2016.

[3] Türk Loydu. S.P 01/20 Guidelines for the Assessment of Sloshing Impact Loads. Technical report. 2020.

[4] Budiansky, B. Sloshing of Liquids in Circular Canals and Spherical Tanks. Journal of the Aero/Space Sciences 1960, 27, 161-173.

[5] Abramson, H. The Dynamic Behavior of Liquids in Moving Containers, with Applications to Space Vehicle Technology. National Aeronautics and Space Administration (NASA). Technical Report. 1966.

[6] Slibar, A.; Troger, H. The Steady State Behaviour of Tank Trailer System carrying Rigid or Liquid Cargo. Vehicle System Dy-namics 1977, 6, 167-169.

[7] Ranganathan, R. Rollover Threshold of Partially Filled Tank Vehicles with Arbitrary Tank Geometry. Journal of Automotive Engineering 1993, 207, 241-244.

[8] Salem, M.I.; Mucino, V. H.; Saunders, E.; Gautam, M.; Lozano-Guzman, A. Lateral sloshing in partially filled elliptical tanker trucks using a trammel pendulum. International Journal of Heavy Vehicle Systems 2009, 16, 207-224.

[9] Celebi, M. S.; Akyildiz, H. Nonlinear modeling of liquid sloshing in a moving rectangular tank. Ocean Engineering 2002, 29, 1527-1553.

[10] Akyildiz, H. A numerical study of the effects of the vertical baffle on liquid sloshing in two-dimensional rectangular tank. Journal of Sound and Vibration 2012, 331, 41-52.

[11] Bulian, G.; Botia-Vera, E.; Mas-Soler, J.; Souto-Iglesias, A.; Castellana, F.; Repeatability and Practical Ergodicity of 2D Slosh-ing Experiments. Proceedings of the Twenty-second International Offshore and Polar Engineering Conference, Rhodes, Greece, June 2012.

[12] Thiagarajan, K.P.; Rakshit, D.; Repalle, N. The air–water sloshing problem: Fundamental analysis and parametric studies on excitation and fill levels. Ocean Engineering 2011, 38, 498-508.

[13] Borg, M. G.; DeMarco Muscat-Fenech, C.; Tezdogan, T.; Sant, T.; Mizzi, S.; Demirel, Y. K. A numerical analysis of dynamic slosh dampening utilising perforated partitions in partially-filled rectangular tanks. Journal of Marine Science and Engineering 2022, 10, 2, 254.

[14] Chanson, H. Application of the method of characteristics to the dam break wave problem. Journal of Hydraulic Research 2009, 47, 41-49.

[15] Ship Structure Committee (SSC). SSC-336 Liquid Sloshing in Cargo Tanks. Technical report. 1990.

[16] ANSYS Inc. FLUENT User's Guide, 5th ed.; ANSYS Inc., Lebanon, NH, 1998.

[17] Seakeeping Committee of the 28th ITTC. Recommended Procedures and Guidelines: Sloshing Model Tests. Technical Report. 2017.